J. Geophys. 47, 184–190, 1980

Journal of Geophysics

Crustal and Upper Mantle Structure

A Model of Electrical Resistivity Beneath NE-Iceland, Correlation With Temperature

M. Beblo[1] and A. Björnsson[2]

[1] Institut für Allgemeine und Angewandte Geophysik, Universität München, Theresienstrasse 41, D-8000 München 2, Federal Republic of Germany
[2] National Energy Authority, Laugavegur 116, Reykjavik, Iceland

Abstract. Short period magnetotelluric measurements (15 s–1 h) were made at 19 sites in NE-Iceland, distributed over the neovolcanic zone and the adjoining older Tertiary flood basalt areas. With model-calculations of one- and two-dimensional resistivity distributions a characteristic model was found for the lower crust and upper mantle. Beneath a thin surface layer the resistivity is 100 Ωm except within the active neovolcanic zone where it is 50 Ωm. This layer extends to a layer with low resistivity of 15 Ωm. The low-resistivity layer is about 5 km thick. The depth of its upper boundary increases from 10 km to about 20 km with increasing distance from the rift axis. The resistivity beneath the low-resistivity layer is about 100 Ωm down to at least 100 km. Comparison of field data with laboratory measurements on conductivity at high temperatures indicates that the low-resistivity layer consists of partially molten basalt at a temperature of 1,000°–1,100° C. The underlying layer very probably consists of partially molten ultramafic rocks and is presumably the uppermost part of the mantle beneath Iceland. The basaltic low-resistivity layer is interpreted as the base of the crust formed by upward movement of the basaltic melt fraction from the mantle.

Key words: Magnetotellurics – Iceland – Electrical model – Crust-mantle interface – Temperature – Partial melting.

Introduction

The electrical resistivity of the earth's interior depends strongly on temperature. It is also related to melt fraction and chemical composition. For a known electrical resistivity distribution – obtained, e.g., by magnetotelluric field measurements – it is therefore possible to determine temperature, melt fraction and chemical composition within the earth within certain assumptions.

In 1977 a magnetotelluric field program was carried out in North and East Iceland in cooperation between the university of Munich, Germany, and the National Energy Authority, Iceland. The aim was to investigate vertical and lateral variations of the electrical resistivity. The measurements were made along two profiles: one 260 km long, east-west, 12 magnetotelluric stations, ranging from the Tertiary flood basalts in North Iceland, across the zone of active rifting and present volcanism, to the Tertiary flood basalts in the eastern part of the country; the other, 150 km long, northeast-southwest, more or less along the neovolcanic zone, with 7 magnetotelluric stations (see Fig. 1 for locations).

Mobile magnetotelluric equipment was used consisting of an electrograph, a fluxgate magnetometer and a tape recorder. Two horizontal components of both the magnetic and the electric field were recorded in the period range of 15 s to 1 h for one or two days at each site.

For more detailed information on the experiment and on the general geological situation the reader is referred to Beblo and Björnsson (1978). They presented the preliminary results of the magnetotelluric measurements on the east-west profile. They used one-dimensional model calculations for constructing a resistivity model of the lower crust and upper mantle.

The most significant result of this work was the existence of a low-resistivity layer (15 Ωm) at about 10–20 km depth. Beblo and Björnsson interpreted this layer as caused by partial melting at the base of the crust.

The present paper discusses the results from all 19 magnetotelluric stations, interpreted with one- and two-dimensional model calculations for the resistivity distribution. The computed resistivities are then compared to resistivities determined in the laboratory on different rock types at high temperatures.

The Magnetotelluric Results

The electrical resistivity of the earth can be determined by the magnetotelluric method, which is based on the observation of time-varying magnetic (**B**) and electric (**E**) fields at the earth's surface. The observed time functions $E(t)$ and $B(t)$ are Fourier-transformed into functions of frequency, from which the complex transfer function C_{ij} can be determined.

$$C_{ij}=\frac{1}{i\omega\mu_0}\cdot z_{ij}, \text{ with impedance } z_{ij}=\mu_0\frac{E_i}{B_j}, \quad \omega=\frac{2\pi}{T},$$

SI units, **B** in nT **E** in mV/km, T in s.

Preference Direction of the Electric Field

Important parameters obtained by the magnetotelluric method are the preference direction and the polarization of the induced electrical field. The polarization (axial ratio of polarization ellipse) is a measure of the surface inhomogeneity of the electrical resistivity distribution at the measuring site. The preference direction (direction of major axis of polarization ellipse) is a function of lateral variations of the electric resistivity in a more regional sense. In the case of a two-dimensional structure with low resistivity in higher-resistivity surroundings the preference direction is parallel to the strike inside the anomalous region and perpendicular to

0340-062X/80/0047/0184/$01.40

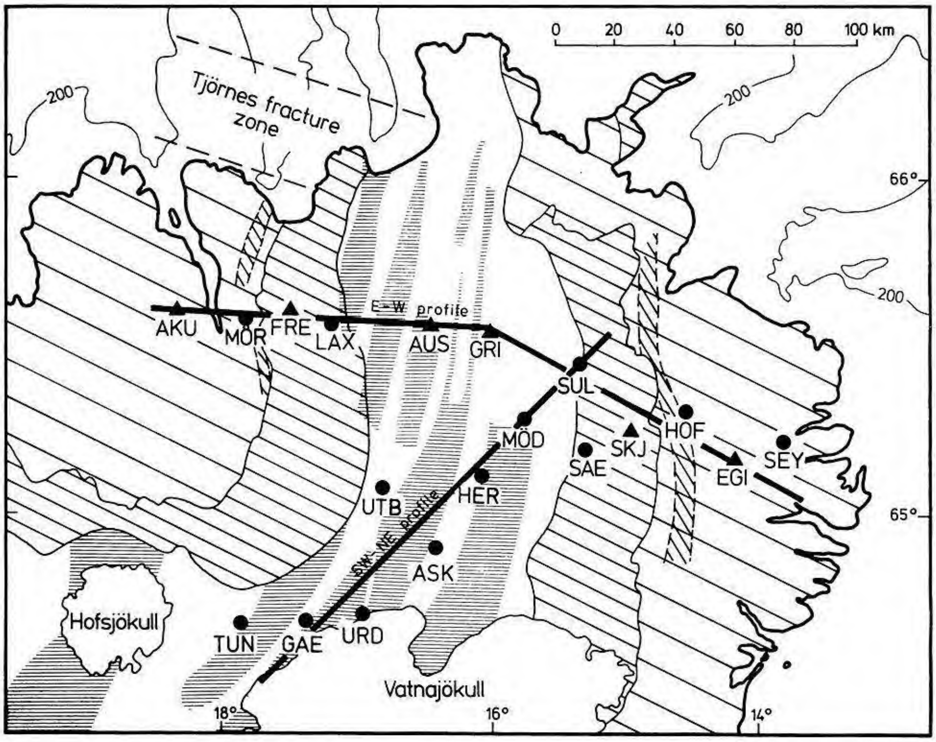

Fig. 1. Simplified geological map of northeast Iceland as redrawn from Saemundsson (1974), showing locations of magnetotelluric measuring stations. Lines are drawn along the two profiles discussed, east-west across the zone of rifting and volcanism, and southwest-northeast along it
Tertiary flood basalt older than 3 m.y.
Quaternary flood basalt 3–0.7 m.y.
Neovolcanic zone younger than 0.7 m.y.
Fissure swarm
Flexured zone
▲ MT-measuring site 15 s–12 h
● MT-measuring site 15 s–1 h

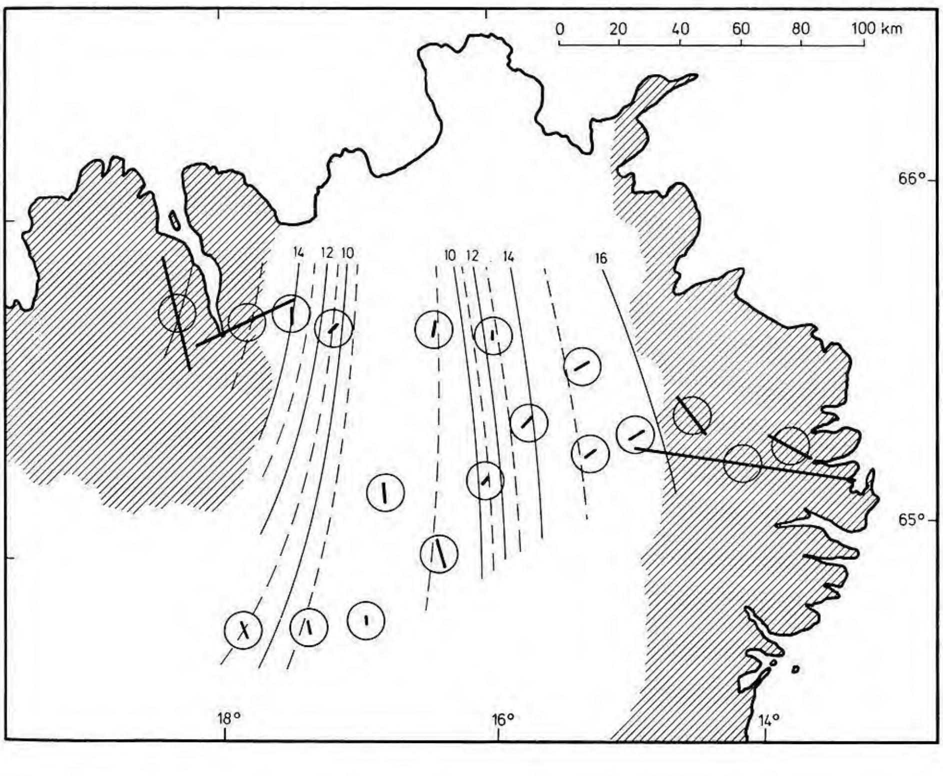

Fig. 2. Preference directions of the induced electrical field for the period range 15–300 s shown by lines in the circles. Depth contour lines of top of the low-resistivity layer; depths in km

the strike outside, an effect of the boundary conditions of the electrical field components at a lateral resistivity contrast.

Figure 2 shows the distribution of the preference direction of the electric field at all magnetotelluric stations for the period range 15 to 300 s. The length of the lines is proportional to the polarization; it should reduce to points for a laterally uniform distribution of resistivity. Within all the Quaternary flood basalt areas and the neovolcanic zone, the short lines indicate small horizontal variations of resistivity. Within the Tertiary flood basalt areas (hatched areas in Fig. 2) there exists a strong horizontal variation of resistivity. The orientation of the preference direction perpendicular to the regional strike outside the Quaternary and the neovolcanic zones and the orientation nearly parallel to the strike inside suggests to us, that within the Quaternary and the

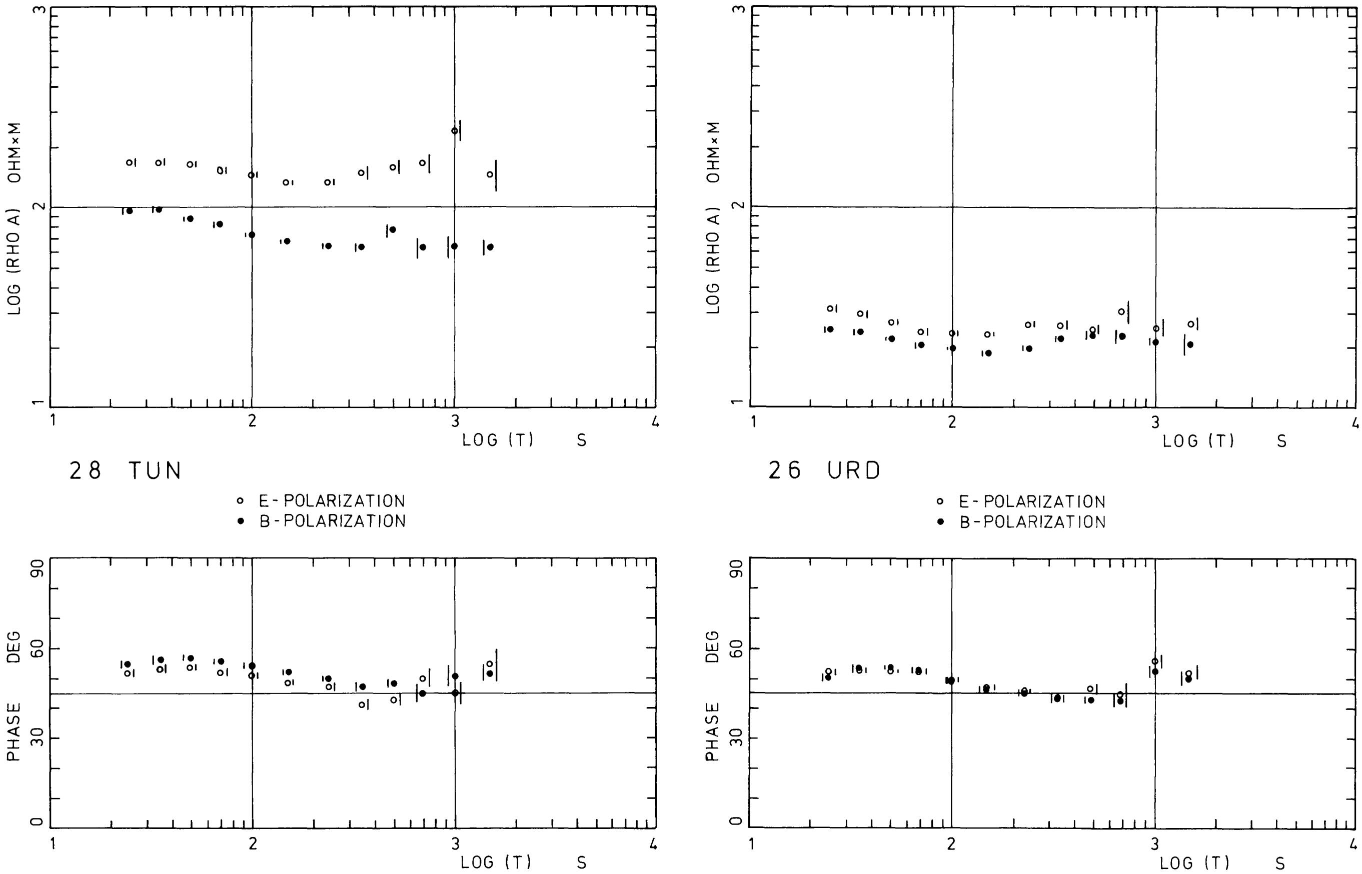

Fig. 3. Apparent resistivities and phase differences (points) and mean square deviations (lines) for the sites *URD* and *TUN*. *E*-and *B*-polarization are nearly identical for *URD*, which implies a one-dimensional resistivity distribution. The difference in *E*- and *B*-polarization at *TUN*, on the other hand, indicates a two- or even three-dimensional resistivity distribution or strong lateral variation in the surface resistivity

neovolcanic regions the surface resistivity is much lower than within the Tertiary basalt areas.

Apparent Resistivities and Phase Differences

Magnetotelluric measurements normally reveal three-dimensional resistivity structures. At the present stage of computer capacities it is not practicable, however, to interpret such structures quantitatively. On the other hand, several methods have been published (e.g., Haak, 1972) for the interpretation of magnetotelluric data in the case of one- or two-dimensional resistivity structures. For a two-dimensional resistivity distribution it is possible to orientate the coordinate system in such a manner, that one axis is parallel and the other perpendicular to the strike of the anomaly. Hence two independent systems of equations are obtained and therefrom two different values for the apparent resistivity ρ_a and phase φ are calculated. The first case means the component of the electric field parallel to the strike (*E*-polarization), the other case means the component perpendicular to the strike (*B*-polarization).

$$\rho_{a_{\parallel}} = \frac{\mu_0 T}{2\pi} |z_{\parallel}|^2, \quad \varphi_{\parallel} = \arg(z_{\parallel}) \quad E\text{-polarization}$$

$$\rho_{a_{\perp}} = \frac{\mu_0 T}{2\pi} |z_{\perp}|^2, \quad \varphi_{\perp} = -\arg(z_{\perp}) \quad B\text{-polarization}$$

ρ in Ωm, φ in degrees.

In the case of a one-dimensional resistivity distribution, both solutions for *E*- and *B*-polarization become identical.

As an example, Fig. 3 shows for the sites Tungnafellsjökull (TUN) and Urdarhals (URD), the calculated values and mean square deviations of the apparent resistivities and phase differences, separately for *E*- and *B*-polarization. The values for the *E*- and *B*-polarization at the site URD are more or less identical, indicating that the resistivity distribution is a function of depth only. At the site TUN polarization of the electrical field is observed, and hence the values for *E*- and *B*-polarization are different. This effect may be caused by a two-dimensional resistivity distribution, or may result from inhomogeneities of surface resistivities (Beblo, 1974). Extremely small deviations of apparent resistivities ρ_a (see Fig. 3) indicate no influences related to an inhomogeneous source field in the observed period range. The ocean effect cannot either be seen in ρ_a, the complete decrease of the ΔZ component of the magnetic field for very long periods (>6 h) (Haak et al., in preparation) supports this.

Model-Calculations

In interpreting magnetotelluric data usually the impedance tensor for model structures is computed and compared to the values obtained from the measurements. The simplest models are one-dimensional, i.e., the resistivity varies only with depth. One-dimensional model-calculations are acceptable, if horizontal variation

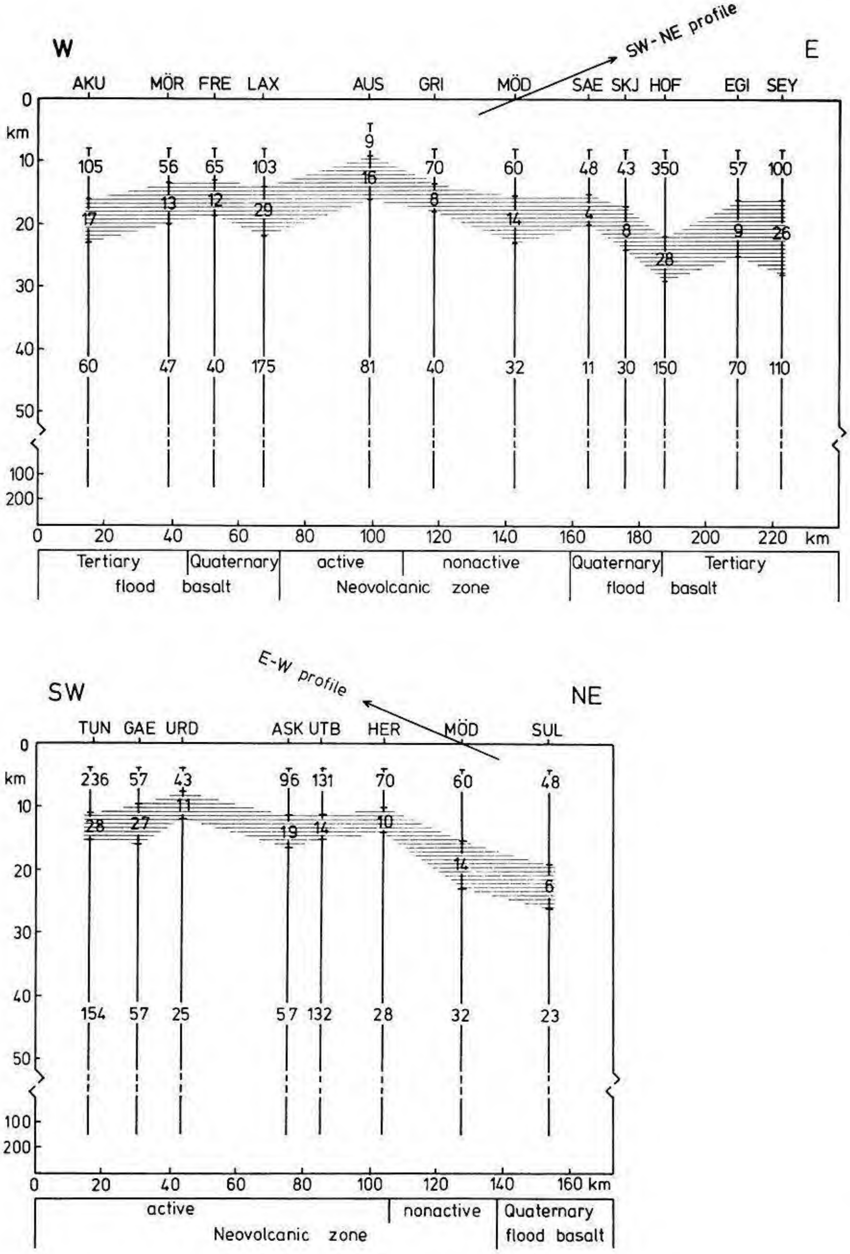

Fig. 4. One-dimensional models of resistivity distribution at all stations, calculated from apparent resistivities and phases of the E-polarization case. The hatched area shows a continuous low resistivity layer with a mean resistivity of 15 Ωm. The numbers indicate resistivities in Ωm, actually computed for each station. For location of sites and profiles see Fig. 1

of resistivity is only weak. From the preference direction (see Fig. 2) this is evident for the measuring sites within the neovolcanic and the Quarternary areas. In the Tertiary areas the preference direction indicates strong horizontal variations in resistivity and one-dimensional model-interpretation is problematic.

However, because of the continuity of the electrical field component parallel to a lateral resistivity contrast, the ρ_a-values of the *E*-polarization case are only weakly influenced by the horizontal near-surface resistivity variations but rather reflect mainly the resistivity variation with depth. Therefore we have used the values of the *E*-polarization for calculating one-dimensional models in the Tertiary areas.

Figure 4 shows the results of the model-calculations for one-dimensional resistivity variation with the depth. For calculating the models we used an inversion method given by Schmucker (1974). For all the stations on both profiles we got the same model type, with the best fit for three-layer models. Although the ρ_a-curves appear extremely flat, the minimum at 100 s and the deviations of the phase from 45° justify at least the use of three-layer models. Models consisting of more than three layers did not show significant improvement in the analyzed period range. Confidence levels computed from the data scatter show model parameter uncertainties less than 10%. Resistivity variations at the surface, which either tend to increase or decrease the resistivity values as a whole in the total period range observed, cause the resistivity values in each layer to vary from station to station but do not weaken the main result. This is stated below.

Beneath the investigated area exists a 5–10 km thick layer with a low resistivity of about 15 Ωm, which is imbedded in layers of higher resistivities. The depth to the low-resistivity layer increases with increasing distance from the spreading axis. Beneath the neovolcanic zone the depth to the well conducting layer is 10 km, but it is about 20 km beneath the Tertiary areas to the east and west. Figure 2 shows smoothed depth contour lines in

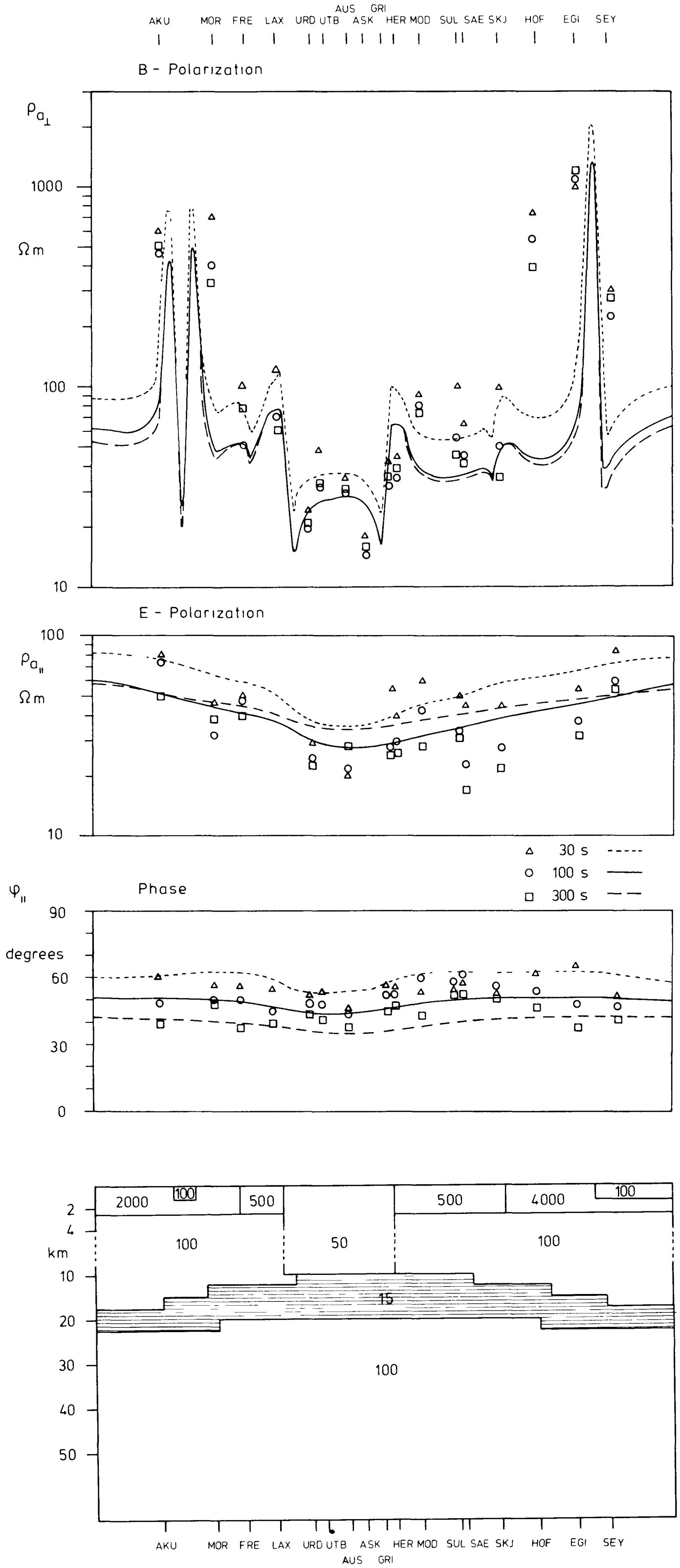

Fig. 5. Two-dimensional model of resistivity distribution beneath east-west profile and computed resistivities and phases for 30, 100, and 300 s. The numbers indicate assumed resistivities in Ωm

km of the top of the low-resistivity layer. The resistivity of the substratum is about 70 Ωm.

Figure 5 shows the results of the model-calculations of a two-dimensional resistivity distribution. The apparent resistivities are shown for both, *B*- and *E*-polarization, the phases are shown for the *E*-polarization case only. For calculating the model curves we used a computer-program by Haak (1978) based on a finite difference method.

The resistivity distribution near the surface has a dominating influence on the *B*-polarization. Hence we formed a near-surface model for the uppermost 2.5 km, based on some resistivity (dipole-dipole) measurements along the profile (Björnsson, 1976). These measurements show high resistivity values for the Tertiary areas (2,000 Ωm in the west, 4,000 Ωm in the east), but much lower resistivities (less than 500 Ωm) within the Quaternary and neovolcanic zones. This near-surface model fits rather well to the *B*-polarization case for all the stations within the Quaternary and the neovolcanic zones. For the Tertiary areas it was not possible to explain the measured values of the *B*-polarization by variation in rock resistivity alone; the computed resistivities are an order of magnitude lower than the observed ones. Therefore we attempted to take into account the influence of the well conducting sea-water in the fjords on both sides of our profile. For the shallow sea-water a resistivity of 100 Ωm has been used according to the model-dimensions. The calculations now show a rather good agreement with the measurements for all the stations over the whole period range. But there remains a deviation which cannot be explained by two-dimensional models and must be caused by three-dimensional local near-surface anomalies (Kemmerle, 1977). This effect can be clearly seen at the site of HOF with calculated $\rho_{a_\perp}$-values an order of magnitude lower than the observed ones. The measuring site of HOF is situated directly in a highly flexured zone near the border of the Tertiary and Quaternary zones (see Fig. 1) which might cause such an effect. A similar, but not as significant deviation can be observed at some other sites, probably caused by near-surface resistivity anomalies as well as by the influence of local topography.

The resistivity distribution at greater depth dominates the *E*-polarization case. Initial guess for two-dimensional model-calculations in greater depth was the result of the one-dimensional model-calculations. These calculations showed a resistivity of about 70 Ωm in the substratum. This resistivity-value fits the *E*-polarization case well, but does not show the weak increase of $\rho_{a_\perp}$ with increasing periods in the *B*-polarization case. A resistivity of 100 Ωm in the substratum gives the observed $\rho_{a_\perp}$-values over the whole period range.

The deviations of the observed $\rho_{a_\parallel}$-values for the *E*-polarization case between adjacent sites are probably produced by small local anomalies of the electrical resistivity near the surface. Such small local anomalies would change the values for the apparent resistivities while the phase difference is obviously not influenced. This can clearly be seen in Fig. 5.

The result of the two-dimensional model-calculations was the following. Below a thin surface layer (2.5 km) the electrical resistivity is 100 Ωm, except within the active part of the neovolcanic zone where the resistivity is 50 Ωm. The layer below has a resistivity of 15 Ωm. The depth to this good conductor increases with distance from the rift axis from 10 km within the neovolcanic zone to about 17 km below the Tertiary basalts. The thickness of the good conductor is 5 km on the eastern and the western side of the profile and about 10 km beneath the Quaternary and the neovolcanic areas. Below the good conductor there is a deep layer with an upper limit of resistivity of 100 Ωm, reaching down

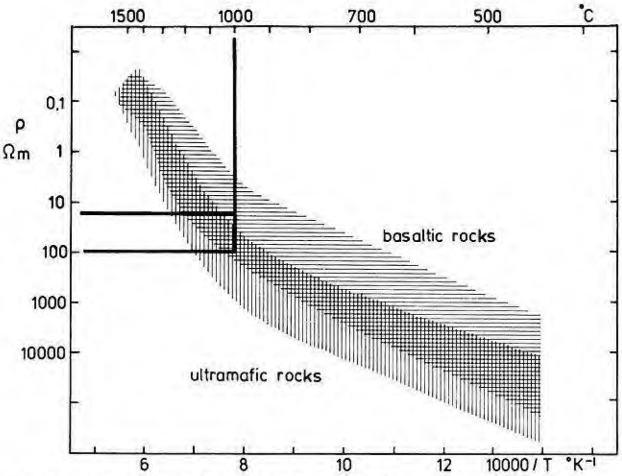

Fig. 6. The electrical resistivity of various basalts and ultramafic rocks as a function of temperature. Redrawn from Haak (1979)

to at least 100 km depth. No exact information can be obtained on the lower boundary of this layer at the present stage, but the deviations of the phase from 45° indicate in the longest periods observed (see Fig. 3) a second good conductor at perhaps 200–300 km depth.

Electrical Resistivity-Temperature

In order to infer the temperature in the lower crust and upper mantle from the resistivity, one must know the dependence of resistivity on temperature for the particular materials of the crust and mantle under the prevailing conditions. In the last few years, a great number of laboratory experiments have been made to investigate the resistivity of different rocks at high temperatures and pressures (for a review see, e.g., Duba, 1976). The most relevant measurements were made on basalts, which are probably the major component of the Icelandic crust. There also exist laboratory measurements on various ultramafic rocks as olivine, which are believed to be the most important component of the upper mantle. Another way to estimate upper mantle resistivity and temperature (done, e.g., by Waff, 1974) is to make theoretical calculations for artificial model-materials, consisting of two different components.

Haak (1979) has given an excellent review of both laboratory experiments and theoretical calculations of electrical resistivity of upper-mantle material. He has collected most of the existing data on basalts and ultramafic rocks. The data scatter considerably and seem to depend strongly on laboratory conditions like oxygen and water fugacities and the measuring technique. Figure 6 is redrawn from Haak (1979) and shows the mean electrical resistivity as a function of temperature for both types of material. There is an overlap in the resistivity distribution of basalts and ultramafic rocks, but it can, nevertheless, be seen that the resistivity of basalt is lower than that of ultramafic rocks at a given temperature by as much as an order of magnitude. For example, the electrical resistivity at 1,000° C is about 15 Ωm for basalts and about 100 Ωm for ultramafic rocks at the same temperature. Figure 6 also shows a significant change in the slopes of the resistivity-temperature curves at about 1,000° C toward lower resistivities above that temperature. This may be caused by the beginning of partial melting.

Discussion

The main result of our investigation is a model of the crust and mantle beneath Iceland, which shows a good conductor at shallow depth. The depth of this layer increases with distance from the rift axis. Since electrical resistivity gives an indication of temperature for a given material, we can discuss the temperatures prevailing in the crust and upper mantle on the basis of the magnetotelluric data; especially the existence or absence of partial melt is in question.

The chemical composition of the lower crust and mantle is not known exactly. But according to most workers it is generally assumed that the crust beneath Iceland consists of basalt and the mantle consists of ultramafic rocks (peridotite). With this assumption we have estimated the temperature by comparing the electrical resistivity inferred from magnetotellurics to the temperature-resistivity curves of Fig. 6.

If the good conductor with a resistivity of 15 Ωm consists of basalt, its temperature should be in the range of 850°–1,200° C with a most likely value near 1,000° C. At this temperature melting begins. Very little can be said about the volume fraction of the melt, but following Shankland and Waff (1977) it could be as much as 10%.

The deeper layer, with a resistivity of about 70–100 Ωm, is believed to be the uppermost mantle, consisting of ultramafic rocks. The corresponding temperature range, according to Fig. 6, is 950°–1,200° C, with a most likely value of about 1,050° C. Some amount of partial basalt melt may be present in a solid olivine matrix. This is supported by seismic observations which indicate anomalously low *P*-wave velocities beneath Iceland (e.g., Tryggvason; 1961; Francis, 1969).

Assuming the 1,000° or 1,100° C isotherm to lie within the good conductor we calculated the mean temperature gradient in the crust (Beblo and Björnsson, 1978). The calculated values showed good agreement with direct temperature gradient measurements in shallow drillholes. The results from the magnetotelluric observations on the SW-NE profile support the earlier interpretation, i.e., a temperature gradient of around 100° C/km in the active zone of rifting and 40°–60° C/km in the Tertiary flood basalt zones to the east and west. No information can be obtained on the temperature gradient in the upper mantle, but the nearly constant resistivity down to 100 km depth indicates a very low temperature gradient for the mantle. This has already been shown by Hermance and Grillot (1974), who found 1° C/km for the temperature gradient within the mantle of SW-Iceland.

It is plausible to interpret the low-resistivity layer to consist of partially molten basalt. This is probably caused by upward movement of lighter basaltic melt through the heavier olivine matrix. The movement causes separation of ultramafic and basaltic material, from which the oceanic crust is generated. A zone of enrichment of partial melt within the oceanic lithosphere has been predicted by Bottinga and Allègre (1976) by theoretical model calculations. They used their result to explain the existence of low-velocity zones near oceanic ridges. Their calculated 1,000° or 1,100° C isotherms are at exactly the depth as our low resistivity layer is. For this depth they predicted a thin zone of enrichment of basaltic composition underlain by ultramafic material. In a recent seismic investigation of Iceland (RRISP-Working Group,

1979) it was found, that the seismic P-wave velocity only slightly increases below 10–15 km depth, velocity reversals were not excluded. Also significantly high values of the P- to S-wave velocity ratio were observed for this depth. Both observations suggest a partially molten state of the mantle beneath Iceland, in good agreement with the magnetotelluric results.

Acknowledgements. The authors are very grateful to Professor Dr. G. Angenheister, Dr. A. Berktold, Dr. V Haak, and Dr. K. Kemmerle for encouragement, support and personal engagement in interpretation and discussion.

References

Beblo, M. Die elektrische Leitfähigkeit unter den Ostalpen, abgeleitet aus magnetotellurischen Messungen längs eines Profiles vom Alpennordrand bis zu den Hohen Tauern. Universität München: Diss. Fak. Geowiss. 1974

Beblo, M., Björnsson, A. Magnetotelluric investigation of the lower crust and upper mantle beneath Iceland. J. Geophys. **45**, 1–16, 1978

Björnsson, A. Electrical resistivity of layer 3 in the Icelandic crust. In· V Greinar ed. pp. 7–23. Reykjavik Societas Scientiarum Islandica 1976

Bottinga, Y., Allègre, C.. Geophysical, petrological and geochemical models of the oceanic lithosphere. Tectonophysics **32**, 9–59, 1976

Duba, A. Are laboratory electrical conductivity data relevant to the Earth? Acta Geodaet. Geophys. Montanist. Acad. Sci. Hung. **11**, 485–495, 1976

Francis, T.J.G. Upper mantle structure along the axis of the Mid-Atlantic Ridge near Iceland. Geophys. J. R. Astron. Soc. **17**, 507–520, 1969

Haak, V Magnetotelluric method The determination of transfer functions in areas with lateral variation of electrical conductivity. Z. Geophys. **38**, 85–102, 1972

Haak, V Interpretations-Verfahren für die Magnetotellurik unter besonderer Berücksichtigung lateral variierender elektrischer Leitfähigkeit im Erdinnern und eines räumlich inhomogenen induzierenden Magnetfeldes. München: Bayerische Adademie der Wissenschaften 1978

Haak, V . Relations between electrical conductivity and petrological parameters of the crust and upper mantle. J. Geomagn. Geoelectr. in press, 1979

Hermance, J.F., Grillot, L.R. Constraints on temperature beneath Iceland from magnetotelluric data. Phys. Earth Planet. Inter **8**, 1–12, 1974

Kemmerle, K. Magnetotellurik am Alpen-Nordrand mit Diskussion der lokalen Effekte und Darstellung einer Einzeleffekt-Auswertung. Universität München: Diss. Fak. Geowiss. 1977

RRISP-Working Group: First results from the Reykjanes Ridge Iceland Seismic Project 1977. Nature **279**, 56–60, 1979

Saemundsson, K. Evolution of the axial rifting zone in northern Iceland and the Tjörnes fracture zone. Bull. Geol. Soc. Am. **85**, 495–504, 1974

Schmucker, U.· Erdmagnetische Tiefensondierung mit langperiodischen Variationen. In: Protokoll DFG-Kolloquium Erdmagn. Tiefensond., A. Berktold, ed.· pp. 313–342. Grafrath-München: 1974

Shankland, T.J., Waff, H.S. Partial melting and electrical conductivity anomalies in the upper mantle. J. Geophys. Res. **82**, 5409–5417, 1977

Tryggvason, E. Arrival times of P-waves and upper mantle structure. Bull. Seismol. Soc. Am. **54**, 727–736, 1961

Waff, H.S.: Theoretical considerations of electrical conductivity in partially molten mantle and implications for geothermometry. J. Geophys. Res. **79**, 4003–4010, 1974

Received April 10, 1979; Revised Version July 6, 1979